ated, β_1 and V_1 must be equal to $n^2\beta_2$ and V_2/n, respectively. Under these conditions, the voltage provided is

$$\Delta V_s = (n-1)V_T \quad (2)$$

For practical implementations of the circuit of Fig. 1, the condition $\beta_1 = n^2\beta_2$ indicates that transistor M1 should be composed of n^2 parallel connected transistors with (W/L) ratio identical to that of M2. Thus, the matching in transconductance parameters and threshold voltages of transistors is improved. Needless to say, an alternative to the above equation consists in using identical M1 and M2 transistors and a current-mirror gain of n^{-2}. On the other hand, to fulfill the relationship $V_1 = V_2/n$, voltage dividers made up of either passive resistors or diode connected transistors can be implemented.

Note that the proposed circuit can maintain a low current level in transistors M1 and M2 to reduce their λ effects, its behaviour can be well represented by the ideal quadratic law, and, simultaneously, has high output drive capability.

A $-nV_T$ extractor can be derived from Fig. 1*a* with minor modifications. Practically the negative level shifter M3-M4 must be substituted by the positive level shifter shown in Fig. 1*b*. Following a similar procedure as above, the output voltage generated by the resulting circuit extractor is exactly equal to $(1-n)V_T$.

A very low impedance exists at output node B of any of the above circuits, because the low output resistance $(1/g_{m3})$ of the source follower appears divided by the gain of the feedback loop. Hence, the output resistance of the extractor results in the order of $[g_0^2/g_m^3]$.

The influence on the circuit performance of transistor second order effects such as mobility degradation, channel length modulation and device mismatching originate deviations of the output voltage from the theoretical result given by eqn. 2. However, if these effects on equations of I_1 and I_2 are included separately, it can be demonstrated that they do not impose more than a few millivolts of discrepancy for typical parameters values [3].

Experimental results: We built the circuit shown in Fig. 1*a* for $n = 2$ using commercial matched MOS transistor array TC4007. The implemented voltage divider consisted of two series diode-connected and matched transistors between V_{DD} and V_{SS}. Transistor M4 was chosen with an equivalent (W/L) ratio five times larger than that of its M2 transistor counterpart. The circuit was measured and Fig. 2 shows the experimental results obtained for different grounded resistor loads connected to node B. The total supply voltage was 8 V. As

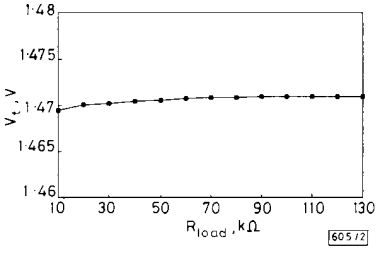

Fig. 2 *Extractor output voltage for different load resistors*

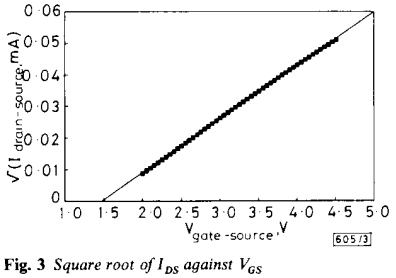

Fig. 3 *Square root of I_{DS} against V_{GS}*

observed, an almost constant V_T value of 1·472 V was provided over this load resistor range. In addition, to examine the validity of these results, we have determined the threshold voltage by means of the classical linear regression method as well. For it, we recorded the I_{DS} of a simple transistor at different V_{GS} voltages. Fig. 3 plots the square root of these measurements. The extrapolated threshold voltage resulting, which would be the crossing of the straight line fit with the horizontal axis, was 1·47243 V showing very good agreement with the voltage generated by the V_T extractor without any measurement or calculation. The coefficient of the correlation provided by the fitting routine was 0·9997.

Conclusions: A $\pm nV_T$ extractor has been presented. Its high accuracy and drive capability has been demonstrated. These features of the proposed circuit should be useful not only for circuit engineers, but also for process engineers.

Acknowledgment: This work was supported by CICYT (Spain) under Grant TIC-91-1059.

11th January 1993

J. F. Duque-Carrillo, J. M. Valverde and R. Pérez-Aloe (*Dept. Electrónica e Ing. Electromed., Universidad de Extremadura, (06071) Badajoz, Spain*)

Reference

1 TSIVIDIS, Y.: 'Operation and modeling of MOS transistor' (McGraw-Hill, New York, 1987)
2 LEE, H.-G., OH, S.-Y., and FULLER, G.: 'A simple and accurate method to measure the threshold voltage of an enhancement-mode MOSFET', *IEEE Trans*, 1982, **ED-29**, pp. 346–348
3 WANG, Z.: 'Automatic V_T extractor based on an $n \times n^2$ MOS transistor array and their application', *IEEE J. Solid-State Circuits*, 1992, **SSC-27**, pp. 1277–1285

NON-VOLATILE MEMORY CHARACTERISTICS OF SUBMICROMETRE HALL STRUCTURES FABRICATED IN EPITAXIAL FERROMAGNETIC MnAl FILMS ON GaAs

J. De Boeck, T. Sands, J. P. Harbison, A. Scherer, H. Gilchrist, T. L. Cheeks, M. Tanaka and V. G. Keramidas

Indexing terms: Epitaxy and epitaxial growth, Memories, Thin-film devices, Magnetic devices and materials

Hall-effect structures with submicrometre linewidths (<0·3 μm) have been fabricated in ferromagnetic thin films of $Mn_{0.60}Al_{0.40}$ which are epitaxially grown on a GaAs substrate. The MnAl thin films exhibit a perpendicular remanent magnetisation and an extraordinary Hall effect with square hysteretic behaviour. The presence of two distinct stable readout states demonstrates the potential of using ultrasmall ferromagnetic volumes for electrically addressable, non-volatile storage of digital information.

Ferromagnetic thin films on semiconductor substrates have recently been used to fabricate non-volatile memories based on their anisotropic magnetoresistive properties [1]. The idea of using the state of the magnetisation in single domain ferromagnetic thin film structures to store binary information is very appealing because of, for example, the inherent non-volatility and hysteretic behaviour. A ferromagnetic thin film with the easy axis of magnetisation normal to the substrate surface will exhibit an extraordinary Hall effect (EHE) when an in-plane current is applied, caused by anisotropic scattering at magnetic moments in the film [2].

Recently, we have demonstrated the molecular beam epitaxial growth and the resulting perpendicular magnetisation

of thin ferromagnetic τ $(MnNi)_xAl_{1-x}$ on AlAs/GaAs [3–5]. In brief, the MBE growth process [6, 7] starts with the room temperature deposition of an amorphous template on an AlAs/GaAs structure. A solid phase crystallisation of the template takes place on heating to ~200°C after which the epitaxial growth of $(MnNi)_xAl_{1-x}$ proceeds by conventional MBE. After completion of the 10 nm thick $(MnNi)_xAl_{1-x}$ film growth, an anneal to 300–450°C is applied to improve the magnetic properties. We have recently discussed the influence of the $(MnNi)_xAl_{1-x}$ alloy composition on the structural and magnetic characteristics of the ferromagnetic film [5].

Fig. 1 demonstrates the EHE ($R_{xy} = V_{xy}/I_{xx} = \rho_{xy}/t$) generated at room temperature in a 12 μm wide $Mn_{0.60}Al_{0.40}$ Hall bar (thickness $t = 10$ nm). The external magnetic field is

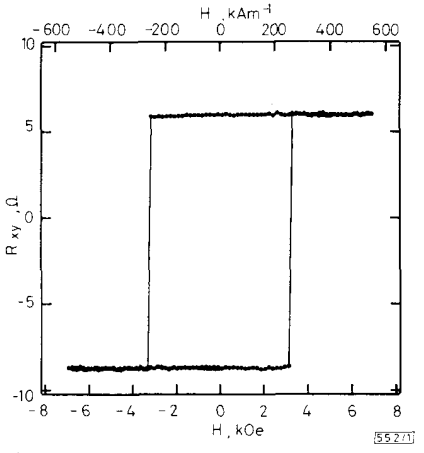

Fig. 1 *Room temperature EHE effect in 12 and 5 μm wide Hall crosses of $Mn_{0.60}Al_{0.40}$ epitaxially grown on AlAs/GaAs*

applied perpendicular to the sample surface in increments of 10 mT and a DC current $I_{xx} = 1$ μA is applied to the Hall bar. An extraordinary Hall voltage results from asymmetric scattering of the carriers at the magnetic sites in the lattice and is many orders of magnitude larger than the Hall voltage generated by the Lorentz force from the external field. The measured ρ_{xy} (7·3 μΩcm) is a materials parameter describing the magnitude of the extraordinary Hall effect. The hysteresis loop is extremely square because the switching to complete saturation occurs within one increment of the applied field, by a domain wall sweeping across the intersection.

The state of the magnetisation in the film can thus be used to store a bit of information [8] with infinite retention time and the information bit can be read nondestructively by sensing the EHE voltage. Writing the information bit then requires the reversal of the magnetisation in the film. A particularly promising aspect of this form of non-volatile storage is that it should be scalable to small sizes in all dimensions. As a first step in the feasibility study of the application of ferromagnetic thin films in future non-volatile memories, we describe the down-scaling of the Hall-structure to submicrometre dimensions in order to obtain ultrahigh packing densities. We demonstrate the fabrication and EHE characteristics of a submicrometre Hall structure that can store a bit of information in a ferromagnetic volume of 300 × 300 × 10 nm³ (0·0009 μm³).

The submicrometre Hall structures are defined by electron beam lithography using an ISI scanning electron microscope. A 140 nm thick SrF_2 mask is fabricated by a standard liftoff procedure and Xe milling is used to pattern the ferromagnetic thin film. The milling is carried out in a UHV etching chamber coupled to the growth chamber of a Riber 1000 MBE system. For passivation purposes, a 20 nm amorphous GaAs layer is deposited on the freshly etched $(MnNi)_xAl_{1-x}$, without leaving the vacuum. A multilegged Hall bar with linewidth of ~300 nm, fabricated in the ferromagnetic τ $Mn_{0.60}Al_{0.40}$, is shown in the SEM picture of Fig. 2. Energy dispersive X-ray analysis has been used to verify the complete removal of MnAl around the small structure.

Fig. 3 shows the EHE hysteresis loop (room temperature, $I_{xx} = 0{\cdot}5$ μA AC) from the Hall cross indicated by the white circle in Fig. 2. The EHE loop of Fig. 3 clearly shows that two

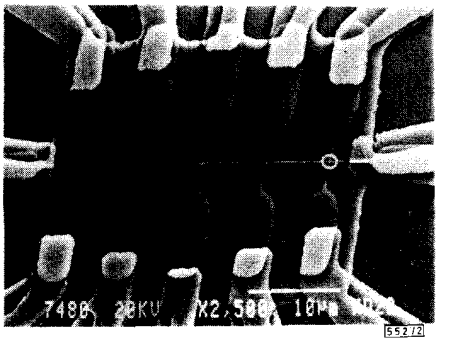

Fig. 2 *SEM micrograph of array of multilegged submicrometre Hall structures fabricated in $Mn_{0.60}Al_{0.40}$/AlAs/GaAs heterostructures*

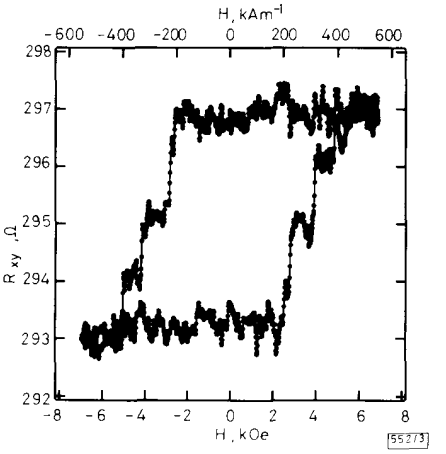

Fig. 3 *Room temperature EHE effect generated in 0·0009 μm³ ferromagnetic volume indicated by the white circle in Fig. 2*

distinct levels remain present in the Hall resistance of these ultrasmall structures, indicating the two stable saturated states of the magnetisation in the 300 × 300 × 10 nm³ volume of the cross. Compared to the EHE loops of the wider structures (Fig. 1) a change in magnetisation reversal and a reduction ($\rho_{xy} = 2$ μΩcm) of the EHE magnitude are observed. Domain walls seem to be stable inside this ultrasmall structure and the magnetisation reversal proceeds in a number of well defined steps. This behaviour is surprising given the fact that a domain wall sweeps rapidly through the 12 μm wide bar. The reduction of the EHE signal, ρ_{xy}, could be caused in part by magnetically inactive material at the edges of the cross as a consequence of the processing. Further, the EHE shows an offset, ~295 Ω in this case, that varies from one Hall cross to another in this multilegged structure. The exact origin of the offset on the EHE voltage is unclear at present, but geometrical asymmetries could become important at these reduced dimensions and we are currently attempting to model the effect of such asymmetries.

Many properties of the present structures are very appealing to high density, semiconductor based non-volatile memory applications: good structural quality of the coherent τ $(MnNi)_xAl_{1-x}$/AlAs/GaAs epitaxial heterostructures, MBE control on uniformity of thickness and alloy composition, room temperature EHE signal, infinite retention time on power loss, magnetic hardness and square hysteresis loops, simplicity and ultrasmall dimensions of the actual memory element and finally, compatibility with existing semiconductor technology. One of the remaining challenges is to find a suit-

able on-chip writing mechanism for these magnetic elements based on for example, Joule heating in combination with a magnetic field from a nearby conductor or current pulse induced domain wall movement [9].

In summary, we have demonstrated submicrometre ferromagnetic structures that can reveal characteristics that are potentially useful for non-volatile memory applications. The readout of these structures can be performed by sensing the extraordinary Hall effect (EHE) voltage, generated by a sense current passed through the perpendicularly magnetised $(MnNi)_xAl_{1-x}$ layer. The actual storage volume is as small as $0{\cdot}0009\ \mu m^3$.

Acknowledgment: J. De Boeck acknowledges partial financial support by NATO.

7th January 1993

J. De Boeck,* T. Sands, J. P. Harbison, A. Scherer, H. Gilchrist, T. L. Cheeks, M. Tanaka,† and V. G. Keramidas (*Bellcore, 331 Newman Springs Rd., Red Bank, NJ 07701, USA*)

* Present Address: Interuniversitary Microelectronics Center, Kapeldreef 75, B 3001 Leuven, Belgium
† On leave from: Dept. Electr. Eng., The University of Tokyo, 7-3-1 Hongo, Bunkyo-ku Tokyo 113, Japan

References

1 DAUGHTON, J. M.: 'Magnetoresistive memory technology', *Thin Solid Films*, 1992, **216**, pp. 162–168
2 DAHLBERG, E. D., RIGGS, K., and PRINZ, G. A.: 'Magnetotransport: an ideal probe of anisotropy energies in epitaxial films', *J. Appl. Phys.*, 1988, **63**, pp. 4270–4275
3 SANDS, T., HARBISON, J. P., LEADBEATER, M. L., ALLEN, S. J., JUN., HULL, G. W., RAMESH, R., and KERAMIDAS, V. G.: 'Epitaxial ferromagnetic τ MnAl films on GaAs', *Appl. Phys. Lett.*, 1990, **97**, pp. 2609–2611
4 LEADBEATER, M., ALLEN, S. J., JUN., DEROSA, F., HARBISON, J. P., SANDS, T., RAMESH, R., FLOREZ, L. T., and KERAMIDAS, V. G.: 'Galvanomagnetic properties of epitaxial MnAl films on GaAs', *J. Appl. Phys.*, 1991, pp. 4689–4691
5 HARBISON, J. P., SANDS, T., DE BOECK, J., CHEEKS, T. L., MICELI, P. F., TANAKA, M., FLOREZ, L. T., WILKENS, B. J., GILCHRIST, H. L., and KERAMIDAS, V. G.: 'MBE growth of ferromagnetic (Mn, Ni)Al on AlAs/GaAs heterostructures'. MBE VII Conf., Schwäbisch Gmünd, Germany, August 24th–28th, 1992 (also to be published *in J. Cryst. Growth*)
6 HARBISON, J. P., SANDS, T., RAMESH, R., FLOREZ, L. T., WILKENS, B. J., and KERAMIDAS, V. G.: 'MBE growth of ferromagnetic metastable epitaxial MnAl thin films on AlAs/GaAs heterostructures', *J. Cryst. Growth* 1991, **111**, pp. 978–981
7 SANDS, T., HARBISON, J. P., ALLEN, S. J., JUN., LEADBEATER, M., CHEEKS, T. L., BRASIL, M. J. S. P., CHANG, C. C., RAMESH, R., FLOREZ, L. T., DEROSA, F., and KERAMIDAS, V. G.: 'Epitaxial τ Mn Al/AlAs/GaAs heterostructures with perpendicular magnetization'. Mat. Res. Symp. Proc., 1992, **231**, pp. 341–346
8 SANDS, T., DE BOECK, J., HARBISON, J. P., SCHERER, A., GILCHRIST, H. L., CHEEKS, T. L., MICELI, P. F., RAMESH, R., and KERAMIDAS, V. G.: 'The extraordinary Hall effect in coherent epitaxial τ (Mn, Ni)Al thin films on GaAs'. 37th Annual Conf. on Magnetism and Magnetic Materials in Houston, Texas, USA, December 1st–4th, 1992, (also to be published in *J. Appl. Phys.*, 1993)
9 BERGER, L.: 'Motion of a magnetic domain wall traversed by fast-rising current pulses', *J. Appl. Phys.*, 1992, **71**, pp. 2721–2726 (and references therein)

ERRATA

ASI, A., and SHAFAI, L.: 'Dispersion analysis of anisotropic inhomogeneous waveguides using compact 2D-FDTD', 1992, **28**, (15), pp. 1451–1452

Authors' corrections

In the third line of the righthand column of p. 1451, the words 'forward difference for' should be deleted

The inline equation after eqn. 3 should read:

$$s = = \frac{c\,\Delta l}{\Delta t} \leq \left[2 + \left(\frac{\beta h}{2}\right)^2\right]^{-1/2} \qquad [6]$$

Additional reference

6 CANGELLARIS, A. C.: 'Numerical stability and numerical dispersion of a compact 2D-FDTD method used for the dispersion analysis of waveguides', *IEEE Microw. Guid. Wave Lett.*, 1993, **3**, (1), pp. 3–5

Printers' corrections

In eqns. 2 and 3, $E_z^n(i, j + \frac{1}{2})$ should read '$E_z^n(i, j + 1)$'